High resolution electronic spectroscopy of 1-aminonaphthalene: S_0 and S_1 geometries and $S_1 \leftarrow S_0$ transition moment orientations

Giel Berden and W. Leo Meerts
Department of Molecular and Laser Physics, University of Nijmegen, 6525 ED Nijmegen, The Netherlands

David F. Plusquellic, Ikuo Fujita, and David W. Pratt
Department of Chemistry, University of Pittsburgh, Pittsburgh, Pennsylvania 15260

(Received 20 July 1995; accepted 7 December 1995)

Fluorescence excitation spectroscopy at both vibrational and rotational resolution has been used to probe the changes in energy, electronic distribution, and geometry that occur when 1-aminonaphthalene (1AN) absorbs light at ~332 nm. The 0_0^0 band of the $S_1 \leftarrow S_0$ transition of 1AN is red shifted by nearly 2000 cm^{-1} with respect to the corresponding band of naphthalene. Additionally, it is mainly b-axis polarized, unlike the corresponding bands of naphthalene and other 1-substituted naphthalenes. Thus, $^1L_a/^1L_b$ state reversal occurs on 1-substitution of naphthalene with an NH_2 group. The S_0 state of 1AN is pyramidally distorted at the nitrogen atom. Additionally, the NH_2 group is rotated by ~20° about the C–NH_2 bond. Excitation of 1AN to the zero-point vibrational level of its S_1 state reduces the C–NH_2 bond length by ~0.2 Å and flattens the NH_2 group along both out-of-plane coordinates. Other vibronic bands in the $S_1 \leftarrow S_0$ transition exhibit significantly different rotational constants, inertial defects, and transition moment orientations. An explanation for these findings is given that is based on the well-known conjugative properties of the NH_2 group in chemically related systems. © *1996 American Institute of Physics.* [S0021-9606(96)04710-3]

INTRODUCTION

A simple rule in electronic spectroscopy is that an electric dipole transition between different molecular orbitals (MOs) is allowed only for those orbitals that are, respectively, symmetric and antisymmetric with respect to reflection through a plane. In that event, the transition moment is perpendicular to that plane.[1] Thus, the lowest $\pi\pi^*$ transition in ethylene is allowed and polarized along the C–C axis whereas the lowest $\pi\pi^*$ transition in benzene is orbitally forbidden, though vibronically allowed.

Complications arise in the application of this rule to larger conjugated systems. Naphthalene is an interesting example.[2] Here, there are two low energy $\pi\pi^*$ excitations in simple Hückel MO theory, one of which is degenerate. The first, $\pi_5\pi_6^*$, is allowed and polarized along the short in-plane axis (y), $^1L_a \leftarrow {}^1A$ in the Platt notation.[3] The second, $\pi_4\pi_6^*$ or $\pi_5\pi_7^*$, also is allowed but polarized along the long in-plane axis (x), $^1L_b \leftarrow {}^1A$. Thus, it was at first sight surprising to learn that the lowest energy $\pi\pi^*$ transition of naphthalene is weak and x-axis polarized whereas the second $\pi\pi^*$ transition is strong and y-axis polarized.[4] We now know that the lowest energy $\pi\pi^*$ transition in naphthalene is to an electronic state (^1L_b) that is a nearly equal mixture of the two degenerate excitations, and that the antisymmetric configuration ($\pi_4\pi_6^* - \pi_5\pi_7^*$) lies at lower energy than $\pi_5\pi_6^*$.[5]

Previous experiments performed by Hollas and co-workers[6,7,8] have shown that this rule also can be applied to substituted naphthalenes in an approximate way. Rotational contour analyses of the 0_0^0 bands of the $S_1 \leftarrow S_0$ transitions of 1- and 2-fluoro, hydroxy, and aminonaphthalene showed that, typically, all bands are in-plane ab hybrid bands owing to the inertial contributions of the substituents. (a and b are the in-plane inertial axes, which are parallel to x and y, respectively, in the parent molecule.) However, 1-substituted naphthalenes exhibit mainly a-type activity whereas 2-substituted naphthalenes exhibit mainly b-type activity. More recent high resolution measurements have confirmed these conclusions for naphthalene[9] and the 1- and 2-fluoro and hydroxynaphthalenes.[10,11,12]

The $S_1 \leftarrow S_0$ transitions of 1-substituted naphthalenes are principally a-type ($^1L_b \leftarrow {}^1A$) because substitution in the 1-position has relatively little effect on the nodal properties of the one-electron MO's of the parent molecule. In contrast, substitution in the 2-position produces a major change in the nodal properties of these MO's. Thus, the $S_1 \leftarrow S_0$ transitions of 2-substituted naphthalenes are principally b-type ($^1L_a \leftarrow {}^1A$) owing to a significant contribution of the $\pi_5\pi_6^*$ excitation to the electronic properties of the S_1 state.[11]

We report here a study of the $S_1 \leftarrow S_0$ electronic spectrum of 1-aminonaphthalene (1AN). Experiments have been performed at both low (~1 cm^{-1}) and high (~10^{-4} cm^{-1}) resolution. The low resolution experiments provide information about the vibrational displacements that occur on $S_1 \leftarrow S_0$ excitation. The high resolution experiments on 1AN and several of its isotopomers provide information about the equilibrium geometries of the two states and the orientations of the $S_1 \leftarrow S_0$ transition moments of different vibronic bands. We find, not unexpectedly, that the NH_2 inversion barrier is significantly lower in the S_1 state than in the S_0 state. But we also find, somewhat to our surprise, that the lowest $\pi\pi^*$ transition of 1AN is principally b-axis polarized, unlike the corresponding bands in naphthalene, 1-fluoronaphthalene, and 1-hydroxynaphthalene. 1-Amino

substitution of naphthalene produces a reversal of the ordering of the ^1L_b and ^1L_a states in the parent molecule. Applying the simple rule, this means that the orbitals between which the lowest energy transition occurs in 1AN are, respectively, symmetric and antisymmetric with respect to reflection in the ac plane, not the bc plane. Finally, we give an explanation for these findings that is based on the well-known conjugative properties of the amino group in chemically related systems.

EXPERIMENT

1AN was studied at low resolution using both fluorescence excitation and resonance-enhanced multiphoton ionization (REMPI) techniques. Both methods utilized a supersonic jet for sample preparation. In the fluorescence excitation experiments, 1AN was seeded into He at various backing pressures and expanded through a 1 mm diam pulsed nozzle operating at 10 Hz. The resulting jet was crossed about 2.5 cm downstream of the nozzle by a doubled Nd^{3+}/YAG-pumped dye laser (FWHM $\sim$0.3 cm^{-1}), also operating at 10 Hz. The resulting fluorescence was collected by a single lens system, focused on a PMT, and detected using a boxcar integrator interfaced to a MASSCOMP MCS561 data acquisition system. Spectra were calibrated in relative frequency to $\pm$0.1 cm^{-1} using markers from a solid étalon. Dispersed fluorescence spectra were obtained using a 0.25 m Jarrell–Ash monochromator with 150 μ slits.

REMPI measurements were performed using a standard pulsed beam laser ionization mass spectrometer with orthogonal molecular beam, laser beam, and linear time-of-flight axes. 1AN was seeded into a pulsed expansion of helium and skimmed before entering the ionization region.[13] A doubled Nd^{3+}/YAG pumped tunable dye laser (FWHM $\sim$0.15 cm^{-1}) operating at 10 Hz was used to excite 1AN in a one-color (1+1) REMPI scheme. Additionally, a KrF excimer laser was used to ionize 1AN via the triplet state in a two-color (1+1) REMPI scheme. Ions corresponding to the mass of 1AN were collected and amplified by a dual microchannel plate detector that was monitored by a 10-bit digital oscilloscope interfaced via a parallel GPIB bus to a personal computer. The PC also controlled the wavelength scans of the dye laser.

1AN was studied at high resolution using fluorescence excitation techniques. The spectrometers employed have been described elsewhere.[9,14] Briefly, a molecular beam formed by expanding 1AN in Ar or He and skimming twice in a differential pumping system was crossed 30 (Nijmegen) or 100 cm (Pittsburgh) downstream of a CW quartz nozzle ($\sim$100 μ diam) with the collimated beam of a CW ring dye laser (FWHM $\sim$500 kHz) operating in the UV. Fluorescence detection using spatially selective optics imaged a small diameter ($\sim$1 mm) portion of the interaction region onto a PMT placed above the crossing point of the two beams. Standard photon counting and data acquisition techniques were employed to record the spectra. These were calibrated to $\pm$1.0 MHz using simultaneously acquired interference fringes from a near-confocal interferometer and the I_2 absorption spectrum.[15] A typical $\sim$5 cm^{-1} scan took 30 min or less and generated 1 Mbyte of data. The computer software that was used to acquire, display, and analyze the high resolution spectra is described elsewhere.[14,16]

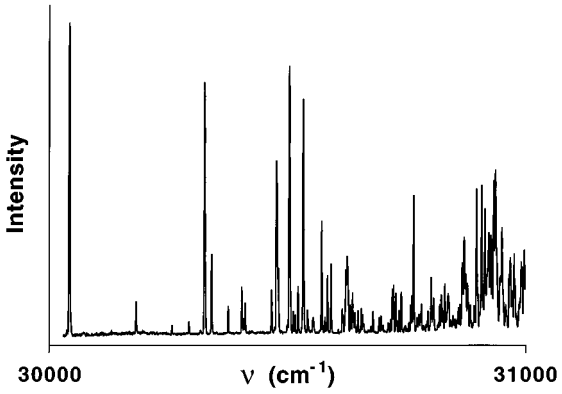

FIG. 1. Fluorescence excitation spectrum of the $S_1 \leftarrow S_0$ electronic transition of 1-aminonaphthalene in a supersonic jet. The origin lies at $\sim$30 044 cm^{-1} ($\sim$333 nm).

Deuterated 1AN was prepared by dissolving 1AN in methylene chloride and mixing the solution with D_2O in a rotating evaporator, with mild heating (35 °C). The resulting deuterated compound was separated from the D_2O and CH_2Cl_2 to give a solid sample.

RESULTS

Figure 1 shows the low resolution $S_1 \leftarrow S_0$ fluorescence excitation spectrum of 1AN recorded in a supersonic jet. The prominent features are a strong band at $\sim$30 044 cm^{-1}, a number of well-resolved vibronic bands at energies up to $\Delta E \sim 600$ cm^{-1} above the apparent origin, and a much higher density of vibronic bands at still higher energies. A list of the stronger observed bands up to $\Delta E = 723$ cm^{-1} is given in Table I. The one- and two-color (1+1) REMPI spectra of 1AN are qualitatively similar to the fluorescence excitation spectrum. A spectrum was measured in a two-color (1+1) REMPI scheme in which the ionization laser was delayed by 500 ns with respect to the excitation laser. Since the lifetime in the S_1 state is only 11 ns (see below), 1AN is ionized from the triplet state. It is therefore concluded that a significant coupling exists between the first excited singlet and triplet states in 1AN.

Representative dispersed fluorescence spectra are shown in Fig. 2. Exciting the band at $\sim$30 044 cm^{-1} results in strong resonance fluorescence and other fluorescence components to lower energies, characteristic of an electronic origin band. Strong bands were observed in this spectrum at displacements of $\Delta E = -467$, -943, -1389, and -1848 cm^{-1}. Weaker emissions were observed between the strong bands. Exciting the $S_1 \leftarrow S_0$ band at $\Delta E = 284$ cm^{-1} results in a similar pattern of intensities, a surprising result if this band is not an origin. "Hot band" dispersed fluorescence spectra (not shown in Fig. 2) are more typical of the vibronic bands of an allowed electronic transition, with a weak–strong–

TABLE I. Prominent bands observed in the $S_1 \leftarrow S_0$ fluorescence excitation spectrum of 1-aminonaphthalene.

Energy	ΔE (cm^{-1})[a]	Int.[b]	Energy	ΔE (cm^{-1})[a]	Int.[b]	Energy	ΔE (cm^{-1})[a]	Int.[b]
29 980.6	−63.0	HB	30 478.4	434.8	55	30 633.8	590.2	9
30 027.0	−16.6	HB	30 480.0	436.4	48	30 638.5	594.9	13
30 043.6	0.0	100	30 482.4	438.8	20	30 642.9	599.3	6
30 088.4	44.8	HB	30 501.8	458.2	2	30 649.6	606.0	7
30 184.0	140.4	10	30 505.5	461.9	85	30 656.5	612.9	8
30 259.2	215.7	3	30 514.0	470.4	7	30 659.9	616.3	6
30 295.0	251.4	4	30 517.7	474.1	6	30 662.0	618.4	3
30 313.4	269.8	HB	30 523.9	480.3	15	30 667.7	634.1	2
30 319.2	275.5	1	30 534.8	491.2	75	30 681.4	637.8	7
30 327.8	284.2	82	30 543.8	500.2	7	30 694.4	650.8	5
30 342.6	299.0	25	30 546.7	503.1	2	30 698.2	654.6	5
30 372.8	329.2	HB	30 550.1	506.5	HB	30 702.5	658.9	2
30 377.3	333.6	9	30 551.8	508.2	1	30 714.2	670.6	3
30 386.2	342.6	HB	30 555.2	511.6	5	30 718.6	675.0	4
30 405.8	362.2	15	30 556.7	513.0	3	30 722.0	678.4	14
30 409.9	366.3	5	30 557.0	513.4	HB	30 724.9	681.3	15
30 413.1	369.5	9	30 573.6	530.0	36	30 729.6	686.0	12
30 445.3	401.7	2	30 580.7	537.1	5	30 732.2	688.6	3
30 449.8	406.2	1	30 585.8	542.2	18	30 736.5	692.9	6
30 451.6	408.0	HB	30 593.4	549.8	22	30 741.1	697.5	13
30 453.3	409.7	4	30 616.6	573.0	7	30 756.6	713.1	3
30 458.0	414.4	3	30 618.4	574.8	6	30 760.5	716.9	8
30 468.4	424.8	14	30 624.3	580.7	21	30 763.1	719.5	11
30 474.6	431.0	2	30 627.0	583.4	24	30 766.4	722.8	45
			30 628.7	585.1	21			

[a]Relative frequencies accurate to ± 0.5 cm^{-1}.
[b]Peak intensities, $\pm 10\%$. HB=hot band.

weak... pattern of intensities. At still higher energies; e.g., $\Delta E = 462$ cm^{-1}; the unusual strong–weak–strong... pattern is again repeated but the most red-shifted bands begin to broaden and merge. We interpret this as evidence for vibrational level mixing, a prerequisite to intramolecular vibrational relaxation. A list of the prominent bands observed in the dispersed fluorescence spectra of 1AN is given in Table II.

Several of the bands in the $S_1 \leftarrow S_0$ excitation spectrum were examined at high resolution. Figure 3 shows the high resolution spectrum of the 0_0^0 band at $\sim 30\,044$ cm^{-1} ($30\,043.60 \pm 0.01$ cm^{-1}), a typical example. The spectrum consists of more than 1000 well-resolved lines, each with a linewidth of 21 MHz (Nijmegen). The minimum linewidth observed for other molecules in Nijmegen is 12 MHz, owing to residual Doppler broadening, transit time effects, fluorescence collection optics, and laser linewidth. From the excess linewidth observed (~ 9 MHz), we estimate the lifetime of S_1 1AN in its zero-point vibrational level (ZPL) to be 11 ± 3 ns. This lifetime is substantially shorter than that of S_1 naphthalene.[9]

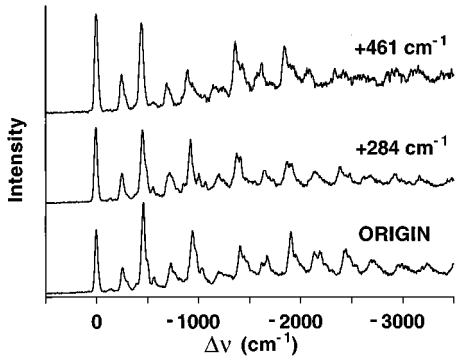

FIG. 2. Fluorescence spectra of selected vibronic bands in the $S_1 \leftarrow S_0$ excitation spectrum of 1-aminonaphthalene.

The spectrum shown in Fig. 3 is predominantly *b*-type; no strong *Q* branches were observed. To fit this band, a spectrum was simulated using asymmetric rotor Hamiltonians for both electronic states, rotational constants estimated from a crude geometrical structure, and the appropriate selection rules. This spectrum was then compared with the experimental one. An initial assignment of lines in the center of the spectrum followed from this comparison. Then, the assigned lines were returned to the fitting program, producing adjustments to the rotational constants and a new simulation. This process was continued until all *b*-type transitions could be accounted for. Still, some unassigned lines appeared in the experimental spectrum. These exhibited patterns characteristic of an *a*-type band. (No other ''extra'' lines were detected.) The observed band is therefore a hybrid band. Including these lines in the fit (a total of 300 assigned lines was used) resulted in a standard deviation of 1.9 MHz, substantially less than the observed linewidth. The parameters determined from this fit are listed in Table III.

A best fit of the observed intensities in the spectrum in Fig. 3 (at $T_r = 3.5 \pm 0.5$ K) yielded a band of $91 \pm 3\%$ *b*-type character and $9 \pm 3\%$ *a*-type character. From the relationship $\tan^2 \theta = I(b)/I(a)$, we calculate $|\theta| = 72° \pm 3°$. Here, θ is the

TABLE II. Prominent bands observed in the $S_1 \rightarrow S_0$ dispersed fluorescence spectra of 1-aminonaphthalene.

Excitation energy (cm^{-1})	ΔE (cm^{-1})[a]	Int.[b]
30 043.6	0	75
(0_0^0)	−141	2
	−262	28
	−307	
	−467	100
	−505	3
	−570	9
	−734	29
	−943	61
	−1032	19
30 088.4	0	43
(0_0^0+45)	−110	87
(Hot)	−246	14
	−357	48
	−567	100
	−680	
	−843	46
	−1057	73
30 327.8	0	92
(0_0^0+284)	−148	1
	−268	34
	−473	100
	−508	46
	−578	11
	−748	30
	−946	61
	−1028	17
30 342.6	0	5
(0_0^0+299)	−329	59
	−600	19
	−792	100
	−1258	
30 386.2	0	
(0_0^0+343)	−880	
(Hot)	−1331	
	−1783	
30 451.6	0	53
(0_0^0+408)	−256	78
(Hot)	−460	49
	−535	49
	−735	85
	−784	100
	−912	52
	−1003	74
	−1378	
30 505.5	0	100
(0_0^0+462)	−262	38
	−463	87
	−586	4
	−717	25
	−922	35
	−1087	9
	−1384	
	−1453	
	−1632	
30 534.8	0	88
(0_0^0+491)	−263	44
	−465	67
	−509	48
	−717	18
	−783	32
	−941	80
	−974	100
	−1017	77
	−1390	
	−1417	
	−1487	
30 550.1	0	100
(0_0^0+507)	−107	27
(Hot)	−256	31
	−359	15
	−477	38
	−563	36
	−722	32
	−1381	
30 557.0	0	69
(0_0^0+513)	−110	100
(Hot)	−256	22
	−356	35
	−480	24
	−576	82
	−821	28
	−1379	
	−1486	
	−1954	

[a]Accurate to ±5 cm^{-1}.
[b]Integrated intensities, ±10%.

angle between the transition moment (TM) vector and the a-inertial axis (positive angles are measured counterclockwise from a), and $I(b)/I(a)$ is the intensity ratio of the a- and b-type bands. The a-axis of 1AN makes an angle of about 16° with the long in-plane axis of naphthalene, x. Thus, the TM vector in 1AN makes an angle of either $\theta' = -56°$ or 88° with the x axis of naphthalene.

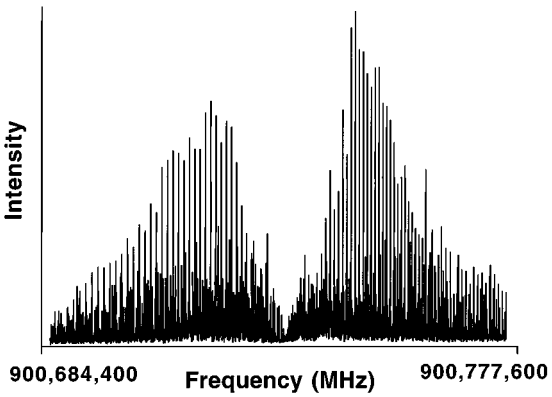

FIG. 3. Rotationally resolved fluorescence excitation spectrum of the electronic origin in the $S_1 \leftarrow S_0$ transition of 1-aminonaphthalene. Note the mainly b-type polarization of the band.

TABLE III. Inertial parameters of the zero-point vibrational levels of the S_0 and S_1 electronic states of 1-aminonaphthalene.

	S_0		S_1
A, MHz	1933.8 (3)	ΔA, MHz	45.61 (2)
B, MHz	1127.6 (2)	ΔB, MHz	−28.19 (1)
C, MHz	713.1 (2)	ΔC, MHz	−5.916 (8)
κ''	−0.321 (1)	κ'	−0.383 (1)
$\Delta I''$, amu Å^2	−0.80 (2)	$\Delta I'$, amu Å^2	−0.37 (2)
	Band origin	30 043.60±0.01 cm^{-1}	
	Band character	91±3% *b*-type, 9±3% *a*-type	

Two additional properties of the data shown in Table III are worthy of note here. The first is that the rotational constant *A increases* on electronic excitation, suggesting a contraction of 1AN in directions perpendicular to *a* with the absorption of a photon. The second is that the magnitude of the inertial defect (ΔI), relatively large in S_0 (−0.80 amu Å^2), *decreases* on $S_1 \leftarrow S_0$ excitation to −0.37 amu Å^2. This suggests that 1AN is distorted from planarity in the ground electronic state along some out-of-plane coordinate(s), and becomes more planar in the S_1 state.

To probe further the atomic displacements responsible for these changes, high resolution experiments also were performed on several deuterated 1AN's. Eight deuterated species resulted when 1AN was exchanged with D_2O; each gave a fully resolved $S_1 \leftarrow S_0$ fluorescence excitation spectrum. However, because each spectrum spans ~5 cm^{-1}, and the ZPL energy shifts on deuteration are comparable to this width, the observed spectrum of the isotopically mixed sample was extremely congested. Nonetheless, it was possible to fit each of the bands separately, by repeating the procedure previously described, yielding a set of S_0 and S_1 rotational constants for each of the observed isotopomers. Then, by comparing the rotational constants of the different isotopomers using Kraitchman's equations (vide infra),[17] we determined which deuterium-labeled molecule was responsible for each observed 0_0^0 band. The results of these determinations are listed in Table IV.

Examination of the data in Table IV shows that the origin bands of most deuterated 1AN's are blue shifted relative to the origin band of the fully protonated molecule. The only exception is the 0_0^0 band of the DHHH isotopomer which is red shifted by −3.58 cm^{-1}. Further examination of these data shows, also, that most shifts are additive. Thus, for example, the shift of the DHHH isotopomer is −3.58 cm^{-1}, the shift of the HHHD isotopomer is 12.11 cm^{-1}, and the shift of the DHHD isotopomer is 8.59 cm^{-1}. The only exception is the shift for DDHH, predicted to be −2.16 cm^{-1} but observed to be 2.99 cm^{-1}. Finally, we note that the shifts for the two-NHD isotopomers are different, −3.58 cm^{-1} (DHHH) and 1.42 cm^{-1} (HDHH).

Several vibronic bands also were examined at high resolution. The data obtained from fits of these bands are sum-

Table IV. Rotational constants of the zero-point vibrational levels of the S_0 and S_1 states of eight deuterated 1AN's and the parent molecule.

		Origin, cm^{-1}	Rotational Constants in MHz					
			A	B	C	ΔA	ΔB	ΔC
	(DHHH)	-3.58	1878.4	1123.5	704.3	42.6	-26.9	-5.8
	(HHHH)	0.0	1933.8	1127.6	713.1	45.6	-28.2	-5.9
	(HDHH)	1.42	1898.3	1108.4	700.7	41.9	-26.5	-5.7
	(DDHH)	2.99	1847.0	1103.9	692.3	38.7	-25.1	-5.7
	(DHHD)	8.59	1817.1	1123.3	695.4	41.5	-27.0	-5.5
	(HHHD)	12.11	1869.9	1127.4	704.2	44.5	-28.3	-5.6
	(HDHD)	13.56	1836.2	1108.4	692.1	40.8	-26.6	-5.4
	(HDDH)	17.65	1898.5	1082.0	690.0	41.8	-25.9	-5.8
	(HDDD)	28.35	1869.9	1099.5	693.2	44.3	-27.6	-5.7

TABLE V. S_1 rotational constants of several vibronic bands of 1AN and its isotopomers.

ΔE, cm^{-1} [a]	A', MHz	B', MHz	C', MHz	ΔI	Band type[b]
0	1979.4	1099.4	707.2	−0.37	91% *b*
140 (141)	1979.1	1099.5	709.2	−2.2	90% *b*
284	1952.2	1102.3	705.1	−0.58	81% *a*
299	1974.8	1100.5	707.9	−1.2	100% *a*
362	1975.1	1099.9	708.9	−2.4	*a*
366	1976.0	1099.8	707.3	−0.73	*b*
425	1965.7	1101.2	707.8	−2.1	*a*
435 (437)	1975.3	1099.4	707.9	−1.7	*b*
462 (463)	1969.8	1100.9	705.9	0.31	50% *b*
542	1972.9	1100.4	707.8	−1.5	67% *a*
583	1965.9	1101.0	708.1	−2.4	57% *a*
585	1967.8	1100.6	708.3	−2.5	100% *a*
723	1962.3	1101.5	706.4	−1.0	*a*
865	1967.8	1100.3	708.0	−2.3	67% *b*
0 (DHHH)	1921.0	1096.6	698.5	−0.39	*b*
′284′ (DHHH)[c]	1899.9	1098.4	697.6	−1.6	*a*
′723′ (DHHH)[c]	1894.7	1101.2	698.0	−1.6	*a*
0 (HDHH)	1940.2	1081.9	695.0	−0.39	*b*
′284′ (HDHH)[d]	1933.4	1083.6	694.2	0.25	*a*

[a]High resolution values, where different from low resolution ones, are shown in parentheses.
[b]Except where specifically noted, the indicated band type is only approximate; all bands are hybrid in character.
[c]Shifted by 2.72 and 2.70 cm^{-1} with respect to the corresponding band in protonated 1AN.
[d]Shifted by 5.37 cm^{-1} with respect to the corresponding band in protonated 1AN.

marized in Table V. All examined bands exhibit ground state rotational constants that are identical, within experimental error (±0.1 MHz), to those of the S_0 ZPL. Hence, all listed bands originate in this level. However, the S_1 rotational constants, inertial defects, and band polarizations vary significantly from band to band, as shown in Table V. Additionally, the band at $\Delta E = 462$ cm^{-1} exhibits significantly larger single rovibronic linewidths, 33 vs 21 MHz.

DISCUSSION

One of the most intriguing results of this study is the finding that the 0_0^0 band of the $S_1 \leftarrow S_0$ transition of 1AN is predominantly *b*-axis polarized. This is an unexpected result. In early studies of the orientations of the electronic transition moments in substituted naphthalenes, Hollas and Thakur[6,7] found that the 0_0^0 bands in the $S_1 \leftarrow S_0$ spectra of 1FN (1-fluoronaphthalene), 1HN (1-hydroxynaphthalene), and 1AN are mainly *a*-type bands whereas the 0_0^0 bands in the $S_1 \leftarrow S_0$ spectra of 2FN, 2HN, and 2AN are mainly *b*-type bands. They concluded that the angle through which the transition moment is rotated away from the long in-plane axis of naphthalene depends mainly on the position of the substituent and not on its chemical nature. The present result shows that this is not the case. The 0_0^0 bands of 1FN and 1HN are predominantly *a*-axis polarized,[10,11] but the 0_0^0 band of 1AN is predominantly *b*-axis polarized.

Simple MO theory provides an explanation for this result. The relevant Hückel MO's of naphthalene are π_4 ($\epsilon_4 = \alpha + \beta$), π_5 ($\epsilon_5 = \alpha + 0.618\ \beta$), π_6^* ($\epsilon_6 = \alpha - 0.618\ \beta$), and π_7^* ($\epsilon_7 = \alpha - \beta$). The S_1 state has its principal parentage in the two degenerate $\pi\pi^*$ one-electron excitations $\pi_4\pi_6^*$ and $\pi_5\pi_7^*$,

$$\psi(S_1) \sim 0.707(\pi_4\pi_6^* - \pi_5\pi_7^*), \tag{1}$$

whereas the S_2 state derives principally from the one excitation $\pi_5\pi_6^*$,

$$\psi(S_2) \sim \pi_5\pi_6^*. \tag{2}$$

The two product wave functions that comprise the S_1 state exhibit oscillating charge distributions that are oriented along the *x* axis, as shown in Fig. 4. However, the magnitude of the transition moment is small owing to a near cancellation of the two components. Thus, while the 0_0^0 band of the $S_1 \leftarrow S_0$ transition of naphthalene is *x*-polarized, it is very weak ($f \sim 0.001$). In contrast, the $S_2 \leftarrow S_0$ transition of naphthalene is *y* polarized (Fig. 4) and the 0_0^0 band is very strong ($f \sim 1$).

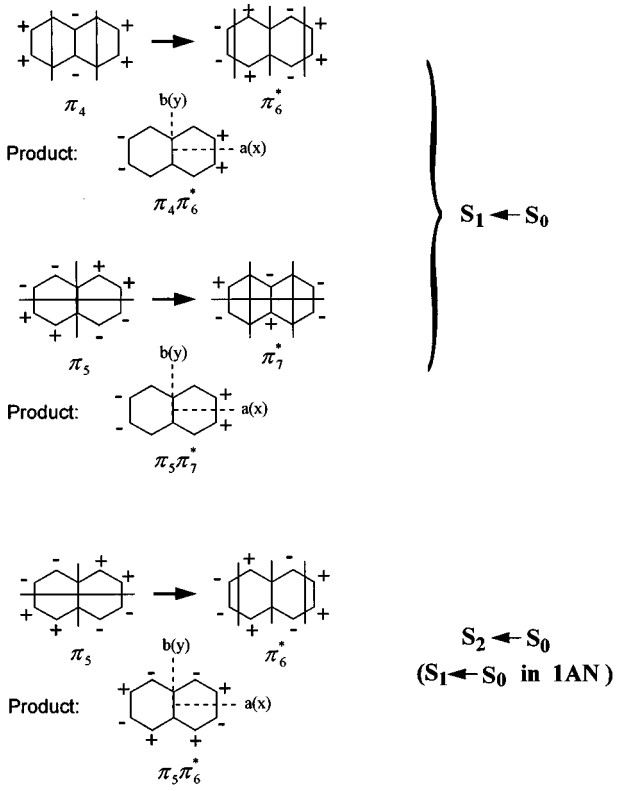

FIG. 4. Hückel molecular orbitals and product wave functions of naphthalene.

The NH_2 group is a powerful activator towards electrophilic aromatic substitution reactions in organic chemistry. In such reactions, this activation is achieved by donation of the lone pair electrons on the basic nitrogen atom to the attached aromatic ring. Typical resonance structures of the carbonium ion formed by *Y*-atom attack para to the NH_2 group of aniline are shown below.[18] Clearly the nitrogen atom can share more than one pair of electrons with the ring by

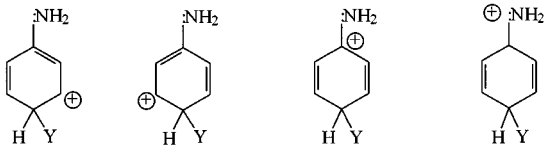

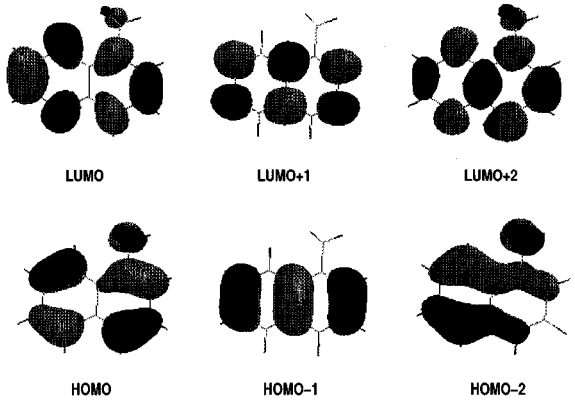

FIG. 5. STO 6-31G* orbitals of 1-aminonaphthalene.

accommodating a positive charge. In 1AN, this donation should affect the energies of both the bonding and antibonding orbitals of the naphthalene chromophore. Since the NH_2 group is strongly ''electron-repelling,'' it *increases* the energies of the bonding orbitals that have large amplitudes at the substituent positions, and it *decreases* the energies of antibonding orbitals that have large amplitudes at the substituent position. The energies of orbitals that have nodes at the substituent position are relatively unaffected.

Applying this argument to 1AN, we see from Fig. 4 that the energy ordering of the relevant MO's should be $\pi_4 < \pi_5$ and $\pi_6^* < \pi_7^*$. This energy ordering is the same as that for naphthalene itself. But, since π_5 is destabilized relative to π_4, and π_6^* is stabilized relative to π_7^*, all one-electron excitations shift to lower energy. The shift of $\pi_5\pi_6^*$ should be twice as large as those of the (still) degenerate excitations $\pi_4\pi_6^*$ and $\pi_5\pi_7^*$. Thus, if the magnitude of the configuration interaction between these two excitations is approximately the same in 1AN as in the parent molecule, the S_1 state in 1AN should derive principally from the configuration $\pi_5\pi_6^*$. In that event, the reflection plane with respect to which the involved orbitals have opposite symmetry in the $S_1 \leftarrow S_0$ transition of 1AN would be the $xz(ac)$ plane (cf., Fig. 4), and the transition would then be y-(b-) axis polarized.

We have performed a series of Hartree–Fock calculations (GAUSSIAN 92, 6-31G* basis set)[19] on S_0 1AN to examine the feasibility of this explanation. Shown in Fig. 5 are approximate pictures of the relevant MO's of the energy-optimized 1AN that were derived from these calculations. 1AN has ten π electrons; additionally, the nitrogen atom contributes a ''lone pair.'' However, examination of this figure shows that, while the nodal patterns of the MO's of naphthalene are largely unperturbed by 1-amino substitution, *all* electrons are extensively delocalized. The energies of the one-electron MO's also are affected. The HOMO-LUMO transition lies at significantly lower energy than either of the now *nondegenerate* (HOMO-1)-LUMO and HOMO-(LUMO+1) transitions. Moreover, Fig. 5 clearly shows that the oscillating charge distribution associated with the HOMO-LUMO transition is oriented close to the b-axis, in accord with the qualitative argument given above. The two higher energy transitions are a-axis polarized. Thus, the $S_1 \leftarrow S_0$ and $S_2 \leftarrow S_0$ transition moment orientations in 1AN are the opposite of those found in naphthalene. This explains the ''anomalous'' polarization of the 0_0^0 band in the $S_1 \leftarrow S_0$ transition of 1AN.

CI-singles calculations, also performed on 1AN using GAUSSIAN 92,[19] confirm this conclusion. The $S_1 \leftarrow S_0$ transition moment is predicted to lie at an angle of 85° with respect to the long in-plane axis of naphthalene. This is in excellent agreement with the measured value of 88°. The calculations also show that while the HOMO-LUMO excitation dominates, the (HOMO-1)-(LUMO+1) excitation also contributes significantly to the $S_1 \leftarrow S_0$ transition.

That ${}^1L_b/{}^1L_a$ reversal might occur on substitution of naphthalene with an amino group was first suggested by Mataga.[20] He found that the solvent shifts of the absorption and fluorescence spectra of naphthylamines were quite different from those of the naphthols, and that the relative magnitudes of the $S_1 - S_0$ dipole moment differences for 1- and 2-derivatives is reversed in naphthylamines when compared with naphthols. Evidence for significant mixing of the L_b and L_a state of naphthylamines also was found in the MO calculations of Suzuki *et al.*[21]

A second relevant observation about the $S_1 \leftarrow S_0$ transition of 1AN is that the 0_0^0 band is significantly red shifted with respect to the corresponding band in naphthalene, by 1975 cm^{-1}. This is the expected result if, as argued above, the affected electrons are significantly delocalized into the NH_2 group. The excited S_1 state should be significantly stabilized relative to the corresponding state in naphthalene. Extending the argument, then, one might expect that other 1-substituted naphthalenes would also exhibit red shifts, that the magnitudes of these shifts would depend on the delocalizing ability of the attached group (i.e., on its chemical nature), and that there would be a correlation between the observed red shifts and band polarizations.

Table VI provides some data that support this view. Listed there are the frequencies of the 0_0^0 bands, the shifts of these bands from the corresponding band in naphthalene, and the observed band polarizations of several 1-substituted naphthalenes.[9–11,22–25] The latter are expressed in terms of the angle (θ') that the TM vector makes with the long in-plane axis (the x-axis in naphthalene) and thus have been corrected for simple inertial effects. Examining the data in this table, we see that the most red-shifted 0_0^0 bands have transition moments that make the largest angles with the x axis, in agreement with the above expectations. Thus, the interaction between the π electrons of naphthalene and the lone pair(s) of the attached substituent is responsible for both the observed red shifts and the observed band polarizations. Notably, the red shift and TM angle are significantly smaller in 1-methylnaphthalene (1MN) than in 1AN. This is reasonable since the methyl group in 1MN, while mildly electron repelling, exhibits only weak hyperconjugation with the aromatic ring.

TABLE VI. 0_0^0 band shifts, $S_1 \leftarrow S_0$ transition moment orientations, and ΔA values of several substituted naphthalenes.

Molecule	Origin, cm^{-1}	Shift, cm^{-1}	TM orientation[a,b]	ΔA, MHz[c]	Ref.
Naphthalene	32 019	⋯	0°	−77.5	9
1FN	31 867	−152	(−)13°	−29.1	10
1HN (*cis*)	31 181	−838	+16°	−23.7	11
1HN (*trans*)	31 455	−564	−17°	−20.5	11,22
1AN	30 044	−1975	+88°	45.6	This work
1MN	31 768	−251	(−)14°	−32.8	23
1CN	31 411	−608	+45°	−21.4	24
1NA	31 074	−945	(−)23,(+)81°	−19.1	25

[a]Angle between the $S_1 \leftarrow S_0$ transition moment vector of 1FN, etc., and the x-(a-) axis of naphthalene. Negative values correspond to clockwise rotation from x.
[b]Absolute signs known only for *cis*-1HN, *trans*-1HN, and 1CN. Other signs based either on a comparison with these values or with theory (1AN).
[c]$\Delta A = A' - A''$.

1HN is a particularly nice example of this effect. Both the *cis* and *trans* isomers exhibit red shifts, larger than that observed in 1FN but smaller than that observed in 1AN. Their TM orientations also are intermediate between those in 1FN and 1AN. Conjugative mixing clearly increases in the order –F, –OH, $-NH_2$. Interestingly, the red shift in *cis*-1HN is 274 cm^{-1} larger than that in *trans*-1HN, and the two transition moments are differently oriented, $\theta' = 16°$ in *cis*-1HN and $\theta' = -17°$ in *trans*-1HN. The difference in red shifts reflects, primarily, a difference in the ground state energies of the two isomers. S_0 *cis*-1HN is ~900 cm^{-1} less stable than S_0 *trans*-1HN,[11] possibly because of the former's nonplanar nature. Recent calculations[26] suggest that the –OH group in S_0 *cis*-1HN is rotated out of the naphthalene plane, possibly because of the steric repulsion from the neighboring (H8) hydrogen atom. Apparently, this effect is small. Recent experiments show that the vibrationally averaged position of the hydroxy–hydrogen atom in *cis*-1HN is "in-plane."[22] Further, the angles of rotation of the TM vectors of *cis*- and *trans*-1HN are comparable in magnitude, though opposite in sign. As discussed elsewhere,[27] the difference in signs reflects primarily the difference in the orientation of the oxygen lone pair orbitals in the two conformers. *Cis/trans* rotation of the OH group rotates the TM vector towards the lone pair electron density on oxygen.

Given the above perspective, substantial geometry changes should occur when 1AN is photoexcited to its S_1 state, especially along coordinates involving the amino group. Indeed, both the $S_1 \leftarrow S_0$ fluorescence excitation and the $S_1 \rightarrow S_0$ dispersed fluorescence spectra of 1AN exhibit pronounced vibrational activity. To set the stage for a meaningful discussion of these results, we begin by describing the key geometrical properties of 1AN, first of the S_0 state.

The principal probes of ground state structure are the S_0 rotational constants of 1AN and its deuterated isotopomers. Kraitchman[17] has given a convenient set of equations that may be used to determine the position of an atom in a molecule. The method utilizes the changes in moments of inertia that are produced when the atom in question is isotopically substituted. To apply the method to 1AN, we first checked the validity of Kraitchman's equations by comparing the rotational constants of the S_0 states of HHHH, DHHH, HDHH, and DDHH isotopomers. This comparison gave two sets of center-of-mass (COM) coordinates of the two NH_2 hydrogens atoms, which agreed within experimental error. Kraitchman's equations are therefore valid. Next, we determined the COM coordinates of the H2 and H4 ring hydrogen atoms by comparing the rotational constants of the S_0 states of the HDHH, HDDH; HDHD, HDDD; HHHH, HHHD; HDHH, HDHD; and DHHH, DHHD isotopomers. The independent determinations (two for H2 and three for H4) again gave identical results. Finally, we determined the positions of all four hydrogen atoms in the energy optimized 6-31G* structure of 1AN, for comparison to experiment. The results of these determinations are listed in Table VII.

Comparing these results, we see that the two aromatic hydrogens are both observed and predicted to lie in the *ab* inertial plane, within experimental error. However, the two NH_2 hydrogens exhibit *nonzero* $|z|$ values. Further, according to experiment, the displacement of the "inside" hydrogen from the *ab* plane is about twice as large as that of the "outside" hydrogen. Two distortions of the ZPL of ground state 1AN are suggested by these results. One is a pyramidalization of the NH_2 group at the nitrogen atom. The second is a rotation of the NH_2 group about the C–NH_2 bond. Supporting evidence for these distortions is provided by the measured inertial defects of 1AN and its isotopomers listed in Table VIII. S_0 1AN in its ZPL has $\Delta I = -0.80$ amu Å^2. (S_0 naphthalene in its ZPL has $\Delta I = -0.2$ amu Å^2.)[9] Deuterium substitution of the NH_2 group in 1AN increases the magnitude of ΔI in the S_0 state. However, the observed increase is position sensitive. The DHHH isotopomer has $\Delta I = -1.27$ amu Å^2, the HDHH isotopomer has $\Delta I = -0.92$ amu Å^2, and the DDHH isotopomer has $\Delta I = -1.14$ amu Å^2. The increase in $|\Delta I|$ is larger for the inside hydrogen than for the outside hydrogen. This shows that the two NH_2 hydrogen atoms in S_0 1AN are inequivalent with respect to reflection through a plane bisecting the NH_2 group, or *diastereotopic*. Similar results have been observed in 2-aminobenzyl alcohol in which the source of the inequivalence is an *intra*molecular hydrogen bond.[28]-

Table VII. Ground state hydrogen atom positions in 1-aminonaphthalene.

H Atom Position	Experimental[a] x(Å)	Experimental[a] y(Å)	Experimental[a] z(Å)	Theoretical (6-31G*) x(Å)	Theoretical (6-31G*) y(Å)	Theoretical (6-31G*) z(Å)
	1.16 (0.03)	2.74 (0.01)	0.49 (0.08)	1.30	2.66	0.68
	2.74 (0.01)	2.24 (0.02)	0.24 (0.17)	2.76	2.22	0.09
	3.36 (0.02)	±0.10 (0.50)	±0.21 (0.25)	3.35	-0.02	-0.01
	0.26 (0.17)	-3.00 (0.02)	±0.14 (0.37)	0.28	-2.98	0.00

[a]Absolute signs based on 6-31G* structure.

The source of the inequivalence of the two NH_2 hydrogens in S_0 1AN is less obvious. One possibility is a difference in the steric interactions between the two NH_2 hydrogens and the adjacent hydrogen atoms of the naphthalene ring, H2 and H8. Experimentally, it is known that the H1–H8 distance is less than the H1–H2 distance in naphthalene, by ~0.05 Å (the *peri* effect).[29] 1AN exhibits the same effect. Figure 6 shows the *ab initio* (6-31G*) structure of 1AN in the vicinity of the attached NH_2 group. Clearly evident is the fact that the two NH_2-ring hydrogen atom distances are different. With the twist angle about the C–NH_2 bond arbitrarily set to zero, the two distances are 1.92 and 2.41 Å. With this constraint relaxed, the two distances are more nearly equal, 2.20 and 2.31 Å. Even in this case, the repulsive interactions between the two NH_2 hydrogens and the ring hydrogens would be different, since the inside hydrogen lies closer to the repulsive wall of H8 than does the outside hydrogen to the repulsive wall of H2. The calculated equilibrium twist angle in S_0 1AN is 20.4°, which gives different $|z|$ values for the two NH_2 hydrogens than are deduced from experiment (Table VII). However, the measured values are subject to vibrational averaging along this (and other) coordinate(s) since they are characteristic of the ZPL level. The remaining theoretical H-atom coordinates are in excellent agreement with experiment (Table VII).

Another property of the 6-31G* geometry of S_0 1AN is an out-of-plane displacement of the nitrogen atom (cf. Fig. 6). The displacement is small, ~0.05 Å with respect to the aromatic plane. Nonetheless, it may contribute to the inertial defect. The calculated inertial defect is larger in magnitude (-1.11 amu Å^2) than that observed experimentally. With this distortion, the calculated NH_2 inversion angle in S_0 1AN is 47.4°.

$S_1 \leftarrow S_0$ excitation of 1AN produces significant changes in the geometry of the molecule. First, we note that ΔA is positive for all examined bands of 1AN; $\Delta A = 45.6$ MHz for the 0_0^0 band. Both ΔB and ΔC are negative. All other naphthalenes examined to date exhibit negative ΔA, ΔB, and ΔC values, as also shown in Table VI (see also Ref. 14). The negative signs are expected. $\pi\pi^*$ excitation typically results in ring expansion, producing increases in the moments of inertia about all principal axes. Since $\Delta A > 0$ in 1AN, one or more bond lengths must decrease, the affected bond(s) being principally perpendicular to a. The logical candidate is the C–NH_2 bond. Contraction of this bond is a natural consequence of the increased electron delocalization in the S_1

Table VIII. Inertial defects (in amu Å^2) of 1AN and its isotopomers in its S_0 and S_1 states.

Band	 S_0/S_1	 S_0/S_1	 S_0/S_1	 S_0/S_1
Origin	-0.80/-0.37	-1.27/-0.39	-0.92/-0.38	-1.14/-0.41
+284 cm^{-1}	-0.80/-0.58	-1.31/-1.61	-0.94/0.25	---
+721 cm^{-1}	-0.82/-1.05	-1.10/-1.58	---	---

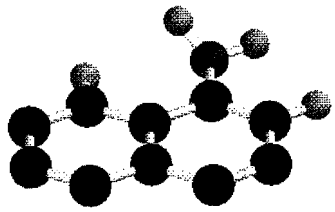

FIG. 6. *Ab initio* geometry of the ground electronic state of 1-aminonaphthalene in the vicinity of the attached NH_2 group. Only the NH_2 and H2 and H8 ring hydrogen atoms are shown.

Table IX. Excited state hydrogen atom positions in 1-aminonaphthalene.

Band						
	x(Å)	y(Å)	z(Å)	x(Å)	y(Å)	z(Å)
Origin	1.05 (0.04)	2.79 (0.01)	0.11 (0.39)	2.69 (0.01)	2.31 (0.02)	0.10 (0.42)
+284 cm^{-1}	1.15 (0.03)	2.74 (0.01)	0.52 (0.08)	2.74 (0.01)	2.24 (0.02)	0.30 (0.13)
+721 cm^{-1}	0.44 (0.09)	2.99 (0.01)	0.53 (0.08)	----	----	----

state. Using the 6-31G* geometry of S_0 1AN, flattened at the NH_2 group, we have determined that a ~50 MHz increase in A requires a decrease in the C–NH_2 bond length of ~0.2 Å. This contraction also affects ΔC because the C–NH_2 bond is nearly perpendicular to both a and c. However, the effect of the shorter bond is especially marked on A rather than C because I_a is less than I_c. In 2AN, the C–NH_2 bond is principally perpendicular to b. Hence, ΔB is positive whereas ΔA and ΔC are negative, as observed by Hollas and Thakur.[6]

We also have determined the COM coordinates of the aforementioned four hydrogen atoms in the S_1 state of 1AN using Kraitchman's equations.[17] The results are listed in Table IX. Comparison of these values with those for the ground state (Table VII) shows some significant differences. The most interesting difference is that, within experimental error, the two NH_2 hydrogens lie in the ab plane in the ZPL level of the S_1 state. Consistent with this finding is the fact that the S_1 inertial defects of the HHHH, DHHH, HDHH, and DDHH isotopomers in this level (Table VIII) are identical, within experimental error, and significantly smaller in magnitude ($\Delta I = -0.37$ amu $Å^2$) than those of the S_0 state. We conclude from these observations that 1AN is a planar (or at least *quasi*planar) molecule in its S_1 state. The two NH_2 hydrogen atoms are "equivalent," or nearly so. Thus, shortening the C–NH_2 bond forces the NH_2 group to adopt a (nearly) coplanar configuration with the aromatic ring. The energy stabilization that results is sufficient to overcome the difference in steric interactions with the adjacent ring hydrogen atoms.

Deuterium substitution of 1AN typically produces blue shifts of the 0_0^0 bands. This is reasonable since, typically, excited state vibrational frequencies are lower than ground state frequencies. The largest shifts observed are for ring atom substitution, 28.35 cm^{-1} in the HHDD molecule. This also is reasonable since ring atom CH frequencies are typically higher than NH_2 group frequencies. Both the signs and magnitudes of these shifts are typical for the delocalized $\pi\pi^*$ states of aromatic molecules.[30] An intriguing result, then, is the finding that the DHHH molecule exhibits a *red* shift, -3.58 cm^{-1}, whereas the HDHH molecule exhibits a *blue* shift, 1.42 cm^{-1}. The inequivalence of the two NH_2 hydrogens is thus apparent even at low resolution. There is a difference in the signs of the vibrational frequency shifts of the inside and outside hydrogens when they are replaced by deuterium. Because DHHH (HDHH) is red (blue) shifted, the substituted hydrogen atom must be distorted along a coordinate whose vibrational frequency increases (decreases) on $S_1 \leftarrow S_0$ excitation.

1AN has 54 normal modes of vibration. According to the 6-31G* calculations, most of these involve displacements of the atoms of the aromatic rings as well as those of the substituent group in the S_0 state. However, a mode at 246 cm^{-1} is principally NH_2 torsional in nature, a mode at 291 cm^{-1} is principally a rocking motion of the NH_2 group, modes at 414 and 618 cm^{-1} contain some NH_2 inversion character, modes at 724 and 741 cm^{-1} contain some NH_2 wagging motion, and a mode at 1647 cm^{-1} is principally a NH_2 scissoring motion. All of these modes are strongly IR allowed. Bands observed in the IR and Raman spectra of 1AN (and their assignments)[31] include fundamentals at 253 cm^{-1} (a'', NH_2 torsion), 660 cm^{-1} (a'', NH_2 wag), 1068 cm^{-1} (a', NH_2 rock), and 1615 cm^{-1} (a', NH_2 scissors). For comparison, Varsanyi's[32] assignments of the corresponding frequencies in aniline are 670 (wag), 1050 (rock), and 1618 cm^{-1} (scissors). We calculate values of 216 (torsion), 638 (wag), 1025 and 1119 (rock), and 1639 cm^{-1} (scissors) using the 6-31G* basis set. (These calculations also show that these vibrations are considerably more localized on the NH_2 group in aniline, compared to 1AN.) Aniline is pyramidally distorted at the NH_2 group with an S_0 inversion barrier of ~526 cm^{-1} and level separations of (0,1)=41, (0,2)=424, and (0,3)=700 cm^{-1}.[33] Its inertial defect in the S_0 state is $\Delta I = -0.405$ amu $Å^2$,[34] substantially less in magnitude than that in S_0 1AN. Thus, with reasonable confidence, we assign the prominent vibrational intervals in the dispersed fluorescence spectra of 1AN to the NH_2 torsional mode (~262 cm^{-1}), two quanta of NH_2 inversion (~467 cm^{-1}), the NH_2 wagging mode (~734 cm^{-1}), the NH_2 rock (~943 cm^{-1}), the C–NH_2 stretch (~1389 cm^{-1}), and the NH_2 scissoring mode (~1898 cm^{-1}). The strongest bands observed are those at (−)467, 943, 1389, and 1848 cm^{-1}. Thus, distortions accompanying $S_1 \rightarrow S_0$ de-excitation are largest along these coordinates, no doubt a consequence of the differing C–NH_2 geometries in the two states.

Little is known about the vibrational bands that appear in the $S_1 \leftarrow S_0$ excitation spectrum of 1AN. Hollas and Thakur[7] observed intense bands in 1AN at $\Delta E = -468.5$, 283.6, and 719.9 cm^{-1}, a pattern similar to that found by Brand *et al.*[35] in the spectrum of aniline (−423, 293, and 760 cm^{-1}). These have been assigned as I_2^0, I_1^1, and I_0^2, respectively, where I is the NH_2 inversion vibration. Mikami *et al.*[36] observed, additionally, bands at 352, 1130, and 1546 cm^{-1} in aniline which they assigned to I_0^1, I_0^3, and I_0^4. An inversion barrier of ~45 cm^{-1} in the S_1 state (ZPE~163 cm^{-1}) was derived from these data. However, some of these latter assignments have been disputed; in particular, I_0^1 and I_0^3 are symmetry forbidden in C_{2v}.[37–39] The current view is that S_1 aniline is a planar molecule with a near-zero inversion barrier. Its S_1 inertial defect is $\Delta I = -0.241$ amu $Å^2$,[34] significantly less than the ground state. As a similar behavior is observed in

1AN, we are tempted to assign the two strong bands at $\Delta E = 284$ and 723 cm^{-1} in the $S_1 \leftarrow S_0$ excitation spectrum as I_1^1 and I_0^2. If these assignments are correct, then one can conclude that the inversion barriers in 1AN are similar to those of aniline, ~ 500 cm^{-1} in the S_0 state and near zero in the S_1 state.

However, we believe the situation in 1AN is more complicated than this. First, we note that since the two H atoms of the NH_2 group are not equivalent, at least in the ground state, the energy surfaces along the inversion and twisting coordinates cannot be symmetric double-well potentials. Second, since the equilibrium geometries of the two electronic states are significantly different, large Duschinsky rotations[40] of the normal modes should accompany $S_1 \leftarrow S_0$ excitation. Third, and most importantly, the polarizations of the observed bands in the fluorescence excitation spectrum vary significantly from band to band. Therefore, one must carefully consider the selection rules for simultaneous rotational, vibrational and electronic (i.e., rovibronic) transitions in 1AN.

If rovibronic wave functions are considered in the first approximation as product functions, and higher order effects (e.g., electrical anharmonicity, Duschinsky rotation, axis tilting, etc.) are neglected, then the transition moment for an electronic transition between two different states may be written as[41]

$$\langle \psi'_e \psi'_v \psi'_r | \mu_Z | \psi''_e \psi''_v \psi''_r \rangle = \sum_g \left\{ \mu_g^0(e',e'') \langle \psi'_v | \psi''_v \rangle + \sum_k [\partial \mu_g(e',e'')/\partial Q_k]_0 \langle \psi'_v | Q_k | \psi''_v \rangle \right\} \langle \psi'_r | \lambda_{Z_g} | \psi''_r \rangle. \quad (3)$$

Here, μ_Z is the component of the electric dipole moment operator along the space-fixed axis Z, μ_g^0 are its projections along the inertial axes $g(=a,b,c)$, with direction cosines λ_{Zg}, and the $[\partial \mu_g(e',e'')/\partial Q_k]_0$ are the dipole derivatives expressed in terms of the normal coordinates of one of the electronic states, evaluated at its equilibrium nuclear configuration. Purely (allowed) electronic transitions are controlled by the first term in the square brackets in Eq. (3), $\mu_g^0(e',e'')\langle \psi'_v | \psi''_v \rangle$, the electronic transition moment multiplied by the vibrational overlap integral. This is the source of the b-type polarization of the 0_0^0 band in the $S_1 \leftarrow S_0$ spectrum of 1AN. This term also can contribute to the intensity of vibronic transitions between two electronic states, but only if the vibrational overlap integral is large. If $\langle \psi'_v | \psi''_v \rangle$ is small, the second term in Eq. (3) will govern the intensity of vibronic transitions. In that event, the polarization of the band will depend upon the direction of the dipole derivative, $[\partial \mu_g(e',e'')/\partial Q_k]_0$. All of this, of course, is well known to those familiar with orbitally forbidden transitions that are vibronically allowed, as in benzene.

Two examples will suffice to illustrate these points. The first strong vibronic band in the $S_1 \leftarrow S_0$ excitation spectrum of 1AN occurs at $\Delta E = 284$ cm^{-1}. It is mainly a-type (81% a). Since this polarization is different from that of the origin band, only the second term in Eq. (3) can contribute to its intensity. Further, the major contributor to this term must be a dipole derivative with a significant projection along a. Among the six possible vibrations of a symmetric NH_2 group,[42] only the rocking and twisting deformation modes would have nonzero dipole derivative projections along the a axis of naphthalene. The inertial defect of 1AN is -0.58 amu $Å^2$ in the upper state vibronic level (Table V), slightly larger in magnitude than that of the S_1 ZPL (-0.37 amu $Å^2$). This changes to -1.6 amu $Å^2$ in the DHHH isotopomer and to 0.25 amu $Å^2$ in the HDHH isotopomer (Table VIII). Since the rocking mode is an in-plane mode and the twisting mode is an out-of-plane mode, the most likely assignment of the band at $0_0^0 + 284$ cm^{-1} is to the twist, or torsional mode in the S_1 state. This frequency is substantially higher than that of the corresponding mode in the ground state, a natural consequence of the enhanced double bond character of the C–NH_2 bond in the S_1 state.

The second strong band in the $S_1 \leftarrow S_0$ excitation spectrum occurs at $\Delta E = 462$ cm^{-1}. It is a hybrid band with $\sim 50\%$ b character and a positive inertial defect ($+0.31$ amu $Å^2$, Table V). Its b-type polarization could derive from either of the two terms in Eq. (3). If the first term contributes, the vibrational overlap integral must be large, suggesting some displacement along this coordinate in the S_1 state. If the second term contributes, the dipole derivative should have a projection along the b axis. Either the wagging or scissoring modes are likely candidates. Of these, only the wagging mode is an out-of-plane mode. This mode has a substantially higher frequency in the ground state (~ 734 cm^{-1}). The a-type polarization of the band at $\Delta E = 462$ cm^{-1} must come from the second term in Eq. (3). Since in-plane vibrations typically make positive contributions to the inertial defect,[17] the most likely source of this intensity is the rocking mode. This mode also has a substantially higher frequency in the ground state (~ 943 cm^{-1}).

While only approximate, other data exist which suggests that an interpretation of this type for the differently polarized vibronic bands is at least conceptually correct. One piece of evidence is the appearance of both red and blue shifts of the 0_0^0 bands of the differently labeled isotopomers of 1AN. Some fundamental vibrational frequencies increase on $S_1 \leftarrow S_0$ excitation whereas others decrease. A second piece of evidence is the unusual patterns that appear in the $S_1 \rightarrow S_0$ dispersed fluorescence spectra of 1AN. Substantial displacements along several vibrational coordinates, probably with significant Duschinsky rotations, are required to account for these observations. That such distortions occur is unambiguously clear from the high resolution data. Finally, since $^1L_b/^1L_a$ state reversal occurs in 1AN, significant vibronic coupling effects may occur low in the S_1 manifold. Thus, a more thorough analysis of the vibrationally resolved spectra of 1AN and its isotopomers will be required to develop a more refined picture of the dynamics that occur on the S_1 PES when the photon is absorbed.

SUMMARY

Several unusual properties of the S_0 and S_1 electronic states of 1-aminonaphthalene (1AN) are revealed by fluorescence excitation experiments in pulsed supersonic jets and CW molecular beams. These properties include their energies, electronic distributions, and geometries; the polarization of the $S_1 \leftarrow S_0$ transition; and the lifetime of the S_1 state. High resolution studies of fourteen vibronic bands in the $S_1 \leftarrow S_0$ fluorescence excitation spectrum of 1AN and several of its isotopomers show that, like aniline, 1AN is pyramidally distorted at the nitrogen atom in the S_0 state, with an inversion angle of $\sim 47°$. However, unlike aniline, the NH_2 group in S_0 1AN also is twisted out of plane by $\sim 20°$, probably because of a difference in the steric interactions between the two NH_2 hydrogens and the adjacent hydrogen atoms of the naphthalene ring (the *peri* effect). The high resolution studies also show that S_1 excitation of 1AN reduces the C–NH_2 bond length by ~ 0.2 Å, providing compelling evidence for enhanced conjugation of the NH_2 group with the π system of the aromatic ring. Shortening the C–NH_2 bond also flattens the NH_2 group and renders the two NH_2 hydrogens equivalent in the S_1 state. The high resolution studies also show that ${}^1L_b/{}^1L_a$ state reversal occurs in 1AN. Thus, the stabilizing influence of the enhanced conjugation is apparently large enough to reorder the energies of the excited states of naphthalene, thereby explaining the unusual polarization of the 0_0^0 band of 1AN, and to overcome the *peri* effect, thereby explaining the unusual characteristics of its vibrationally resolved $S_1 \leftrightarrow S_0$ spectra.

ACKNOWLEDGMENTS

We are grateful for financial support from the Dutch Foundation for Fundamental Research on Matter (FOM) and the U.S. National Science Foundation (CHE-9224398). Calculations were performed at the Pittsburgh Supercomputing Center. We thank J. M. Hollas, L. H. Spangler, and K. Zachariasse for helpful discussions.

[1] J. P. Lowe, *Quantum Chemistry*, 2nd ed. (Academic, San Diego, 1993).
[2] For a review, see L. Salem, *The Molecular Orbital Theory of Conjugated Systems* (Benjamin, New York, 1966).
[3] J. R. Platt, J. Chem. Phys. **17**, 484 (1949).
[4] D. S. McClure, J. Chem. Phys. **22**, 1668 (1954).
[5] M. J. S. Dewar and H. C. Longuet-Higgins, Proc. Phys. Soc. (London) **67**, 795 (1954).
[6] J. M. Hollas and S. N. Thakur, Mol. Phys. **25**, 1315 (1973).
[7] J. M. Hollas and S. N. Thakur, Mol. Phys. **27**, 1001 (1974).
[8] J. M. Hollas and M. Z. bin Hussein, J. Mol. Spectrosc. **127**, 497 (1988).
[9] W. A. Majewski and W. L. Meerts, J. Mol. Spectrosc. **104**, 271 (1984).
[10] W. A. Majewski, D. F. Plusquellic, and D. W. Pratt, J. Chem. Phys. **90**, 1362 (1989).
[11] J. R. Johnson, K. D. Jordan, D. F. Plusquellic, and D. W. Pratt, J. Chem. Phys. **93**, 2258 (1990).
[12] B. B. Champagne, J. F. Pfanstiel, D. W. Pratt, and R. C. Ulsh, J. Chem. Phys. **102**, 6432 (1995).
[13] M. G. H. Boogaarts, P. C. Hinnen, and G. Meijer, Chem. Phys. Lett. **223**, 537 (1994).
[14] W. A. Majewski, J. F. Pfanstiel, D. F. Plusquellic, and D. W. Pratt, in *Laser Techniques in Chemistry*, edited by A. B. Myers and T. R. Rizzo (Wiley, New York, 1995), p. 101.
[15] S. Gerstenkorn and P. Luc, *Atlas du Spectroscopie d'Absorption de la Molecule d'Iode* (CNRS, Paris, 1978).
[16] G. Berden, Ph.D. thesis, U. Nijmegen, 1995.
[17] W. Gordy and R. L. Cook, *Microwave Molecular Spectra*, 3rd ed. (Wiley–Interscience, New York, 1984).
[18] R. T. Morrison and R. N. Boyd, *Organic Chemistry* (Allyn & Bacon, Boston, 1966).
[19] GAUSSIAN 92/DFT, Revision G.3, M. J. Frisch, G. W. Trucks, H. B. Schlegel, P. M. W. Gill, B. G. Johnson, M. W. Wong, J. B. Foresman, M. A. Robb, M. Head-Gordon, E. S. Replogle, R. Gomperts, J. L. Andres, K. Raghavachari, J. S. Binkley, C. Gonzalez, R. L. Martin, D. J. Fox, D. J. Defrees, J. Baker, J. J. P. Stewart, and J. A. Pople (Gaussian, Inc., Pittsburgh, PA, 1993).
[20] N. Mataga, Bull. Chem. Soc. Jpn. **36**, 654 (1963).
[21] S. Suzuki, T. Fujii, and H. Baba, J. Mol. Spectrosc. **47**, 243 (1973).
[22] S. J. Humphrey and D. W. Pratt (unpublished).
[23] X.-Q. Tan, W. A. Majewski, D. F. Plusquellic, and D. W. Pratt, J. Chem. Phys. **94**, 7721 (1991).
[24] G. Berden, W. L. Meerts, and W. Kreiner, Chem. Phys. **174**, 247 (1993).
[25] S. Jagannathan and D. W. Pratt, J. Chem. Phys. **100**, 1874 (1994).
[26] K. D. Jordan *et al.* (unpublished).
[27] P. A. Hepworth, J. McCombie, J. P. Simons, J. F. Pfanstiel, J. W. Ribblett, and D. W. Pratt, Chem. Phys. Lett. **236**, 571 (1995).
[28] J. I. Seeman, H. V. Secor, H.-S. Im, and E. R. Bernstein, J. Am. Chem. Soc. **112**, 7073 (1990).
[29] C. P. Brock and J. Dunitz, Acta Crystallogr. B **38**, 2218 (1982).
[30] See, for example, G. C. Nieman and D. S. Tinti, J. Chem. Phys. **46**, 1432 (1967).
[31] R. D. Singh, O. P. Sharma, H. S. Bhatti, and N. V. Unnikrishnan Nair, Ind. J. Pure Appl. Phys. **20**, 635 (1982); R. Shanker, R. A. Yadav, I. S. Singh, and O. N. Singh, Pramăna **24**, 749 (1985).
[32] G. Varsanyi, *Assignments for Vibrational Spectra of Seven Hundred Benzene Derivatives* (Wiley, New York, 1974).
[33] R. A. Kydd and P. J. Krueger, Chem. Phys. Lett. **49**, 539 (1977).
[34] W. E. Sinclair and D. W. Pratt (unpublished). See also D. G. Lister and J. K. Tyler, Chem. Commun. **1966**, 152; B. Kleiboemer and D. H. Sutter, Z. Naturforsch. **43a**, 561 (1988); E. R. Th. Kerstel, M. Becucci, G. Pietraperzia, and E. M. Castellucci (unpublished).
[35] J. C. D. Brand, D. R. Williams, and T. J. Cook, J. Mol. Spectrosc. **20**, 359 (1966); see also J. Christoffersen, J. M. Hollas, and G. H. Kirby, Mol. Phys. **16**, 441 (1969).
[36] N. Mikami, A. Hiraya, I. Fujiwara, and M. Ito, Chem. Phys. Lett. **74**, 531 (1980).
[37] J. M. Hollas, M. R. Howson, T. Ridley, and L. Halonen, Chem. Phys. Lett. **98**, 611 (1983).
[38] E. R. Bernstein, K. Law, and M. Schauer, J. Chem. Phys. **80**, 207 (1984).
[39] S. Yan and L. H. Spangler, J. Chem. Phys. **96**, 4106 (1992).
[40] F. Duschinsky, Acta Physicochim. U.R.S.S. **7**, 551 (1937).
[41] D. Papoušek and M. R. Aliev, *Molecular Vibrational-Rotational Spectra* (Elsevier, Amsterdam, 1982).
[42] R. T. Conley, *Infrared Spectroscopy* (Allyn and Bacon, Boston, 1966).